Hindawi Publishing Corporation
International Journal of Antennas and Propagation
Volume 2011, Article ID 937261, 8 pages
doi:10.1155/2011/937261

Research Article

An External Calibration Method for Compensating for the Mutual Coupling Effect in Large Interferometric Aperture Synthesis Radiometers

Jian Dong,[1] Ronghua Shi,[1] Ke Chen,[2] Qingxia Li,[2] and Wentai Lei[1]

[1] *School of Information Science and Engineering, Central South University, Changsha 410083, China*
[2] *Department of Electronics and Information Engineering, Huazhong University of Science and Technology, Wuhan 430074, China*

Correspondence should be addressed to Jian Dong, dongjian@mail.csu.edu.cn

Received 30 May 2011; Revised 25 July 2011; Accepted 26 July 2011

Academic Editor: Hon Tat Hui

This paper deals with the antenna mutual coupling effect in interferometric aperture synthesis radiometers (IASRs), which degrades the system radiometric performance. First, the conventional mutual impedance (CMI) is adopted to analyze the mutual coupling effect on the performance of IASR and a practical model of the coupled visibilities is developed. Based on the model, an external calibration method is then proposed to compensate for the mutual coupling effect. In this method, the measured visibilities are decoupled through the difference measurement between the original scene and a naturally occurring reference scene. Compared to the previous methods, the proposed method requires no extra additional hardware cost and has easier implementation and, therefore, fits for the large interferometric array radiometers. Experimental results validate the effectiveness of the proposed method.

1. Introduction

Interferometric aperture synthesis technique, first used in the radio astronomy community [1], has been introduced into passive microwave remote sensing of the Earth with high spatial resolution since the 1980s [2–5]. In an aperture synthesis microwave radiometer, a large antenna aperture can be synthesized by sparsely arranging a number of small aperture antennas and measuring the coherent product (cross correlation) of the signals collected from pairs of antennas at various spacings. The avoidance of the very large and massive mechanical scanning antenna is the main advantage of an aperture synthesis radiometer compared to a conventional real aperture radiometer [6]. However, the use of a number of small aperture antennas may introduce some system radiometric errors and degrade the system radiometric accuracy because of antenna imperfections such as the antenna mutual coupling, antenna pattern ripples, and antenna position errors [7]. Thus, accurate characterization and effective compensation of antenna imperfections is one of the important factors to consider in the design of ISAR. In this paper, the antenna mutual coupling effect will be mainly addressed.

In some interferometric radiometry fields, that is, radio astronomy, the effect of antenna mutual coupling is usually negligible due to the very directive antennas and the very large distance between the antennas. On the other hand, interferometric radiometers for Earth observation require closely spaced antennas with a large half-power beamwidth to deal with the large field of view (FOV) without imaging aliasing. In this case, the effect of antenna mutual coupling is a main source of system radiometric errors. In [8], it is stated that the interferometric pattern in the ESTAR uni-dimensional interferometric radiometers is not sinusoidal because of antenna mutual coupling and multiple reflections in the array structure. Errors are analyzed through the distorted interferometric patterns and calibrated by the G-matrix inversion method [9]. However, due to the need of the accurate measurement of the system impulse response (i.e., the G matrix) and therefore the large extra hardware cost, this method is usually unfeasible for large or two-dimensional spaceborne or airborne IASR systems with

many antennas such as MIRAS [10, 11] and GeoSTAR [12, 13]. Moreover, the matrix inverse operation in this method needs high computational load especially for large interferometric array radiometers with many antennas. Also, Le Vine and Weissman [14, 15] discussed the role of antenna mutual coupling on the performance of synthetic aperture radiometers from the aspects of antenna patterns and interferometric patterns and presented an approach to the measurement of mutual coupling by employing an internal reference source network and an active element antenna. A problem of this approach lies in the additional hardware cost which will increase with the number of antenna elements. Later, Camps et al. [16, 17] tried to compensate for the antenna mutual coupling errors using the conventional mutual impedance (CMI). However, the measurement or computation of the impedance matrix remains a problem, which is usually difficult and time consuming especially for large antenna arrays with complex antenna structures or irregular arrangement.

Following the developments of [16, 17], an external calibration method for compensating the mutual coupling effect is proposed in this paper. In this method, the antenna mutual coupling effect is incorporated into the measured visibility model, and then the visibilities are decoupled through the difference measurement between the original scene and the reference scene. Compared to the previous methods, the proposed method requires no additional hardware cost and has easier implementation and especially fits for the large interferometric array radiometers.

The paper is organized as follows. In Section 2, the effect of antenna mutual coupling on the performance of IASR is analyzed using the CMI. Based on the analysis, in Section 3, the IASR system output (i.e., the visibility function) is modeled and an external calibration method is proposed in order to decouple the measured visibility samples. In Section 4, experimental results are provided to illustrate the effectiveness of the proposed method. Finally, Section 5 sums up the paper and presents conclusions.

2. The Analysis of Antenna Mutual Coupling Effect Using the CMI

Existence of the mutual coupling effect in antenna array has been well known throughout the years, and extensive work has already been contributed to either reducing or compensating such undesirable effects. Among the work, the CMI method [18] has become the most popular method for antenna mutual coupling analysis as mutual impedance can be measured directly or obtained indirectly from the measurement of the S-parameters. Gupta and Ksienski [19] used a circuit theory approach based on the use of the CMI to analyze the effect of antenna mutual coupling on the performance of adaptive arrays. Later, Yeh et al. [20] applied the CMI to decouple the voltages measured from the antenna terminals of a receiving antenna array in a direction-of-arrival (DOA) estimation application. The results with better accuracies of DOA estimation demonstrate that the undesirable mutual coupling effect can be partially compensated via a decoupling process with the CMI. For Earth remote sensing applications, Camps et al. [16, 17] first introduced the CMI method to analyze the effect of antenna mutual coupling on the performance of interferometric aperture synthesis radiometers. In this paper, we will follow the developments of [16, 17] and establish the model of the coupled visibilities.

Figure 1 shows the circuit model of an N-element antenna array. The array is treated as a multiport where each port corresponds to an antenna. According to the model, the relationship between the "load" and the "ideal" voltages is given by

$$\mathbf{v}^L = \mathbf{C}^{-1}\mathbf{v}^o, \tag{1}$$

where $\mathbf{v}^L = [v_1^L, v_2^L, \ldots, v_N^L]^T$, where v_i^L, $i = 1, 2, \ldots, N$ is the voltage measured at the load connected to the port i affected by load mismatch and coupling, the superscript "T" denotes the transpose operation; while $\mathbf{v}^o = [v_1^o, v_2^o, \ldots, v_N^o]^T$, where v_i^o, $i = 1, 2, \ldots, N$ is the voltage that would be measured at the port i when all the antennas are open circuited. The "load" and ideal "o" voltages are related by the impedance matrix

$$\mathbf{C} = \begin{bmatrix} 1 + \dfrac{Z_{11}}{Z_{L1}} & \dfrac{Z_{12}}{Z_{L2}} & \cdots & \dfrac{Z_{1N}}{Z_{LN}} \\ \dfrac{Z_{21}}{Z_{L1}} & 1 + \dfrac{Z_{22}}{Z_{L2}} & \cdots & \dfrac{Z_{2N}}{Z_{LN}} \\ \cdots & \cdots & \ddots & \cdots \\ \dfrac{Z_{N1}}{Z_{L1}} & \dfrac{Z_{N2}}{Z_{L2}} & \cdots & 1 + \dfrac{Z_{NN}}{Z_{LN}} \end{bmatrix}, \tag{2}$$

where Z_{Li} $(i = 1, 2, \ldots, N)$ is the load impedance; Z_{ii} and Z_{ij} $(i, j = 1, 2, \ldots, N)$ are the measured input and mutual impedances, respectively, taking into account the effect of mechanical structure and antenna coupling, and their values depend on the array geometry as well as on the antenna distance and the number of antennas and must be measured when all the antennas are located in the array.

The IASR system output, that is, the visibility function, is a set of complex cross correlation of the voltages collected between various pairs of antennas in an array. Consequently, the measured and ideal visibilities are related by [14, 15]

$$\mathbf{V}^L = \mathbf{C}^{-1}\mathbf{V}^o\left(\mathbf{C}^{-1}\right)^H, \tag{3}$$

where $\mathbf{V}^L = [V_{ij}^L]$ $(i, j = 1, 2, \ldots, N)$ are the measured visibilities between antennas i-j with antenna coupling errors; $\mathbf{V}^o = [V_{ij}^o]$ are the ideal visibilities; the superscript "H" denotes the conjugate transpose operation. Equation (3) reveals that the measured visibilities are a linear combination of all the visibilities that can be synthesized by the array, enlarging the spatial frequency bandwidth, by transferring power from the smallest baselines to the larger ones, and inducing high-frequency artifacts in the recovered brightness temperature distribution [21]. Theoretically speaking, the decoupled visibilities can be obtained from the coupled ones if we manage to compute or measure the $\mathbf{C}$ matrix. However, the measurement or computation of the $\mathbf{C}$ matrix is usually difficult and time consuming especially for large arrays

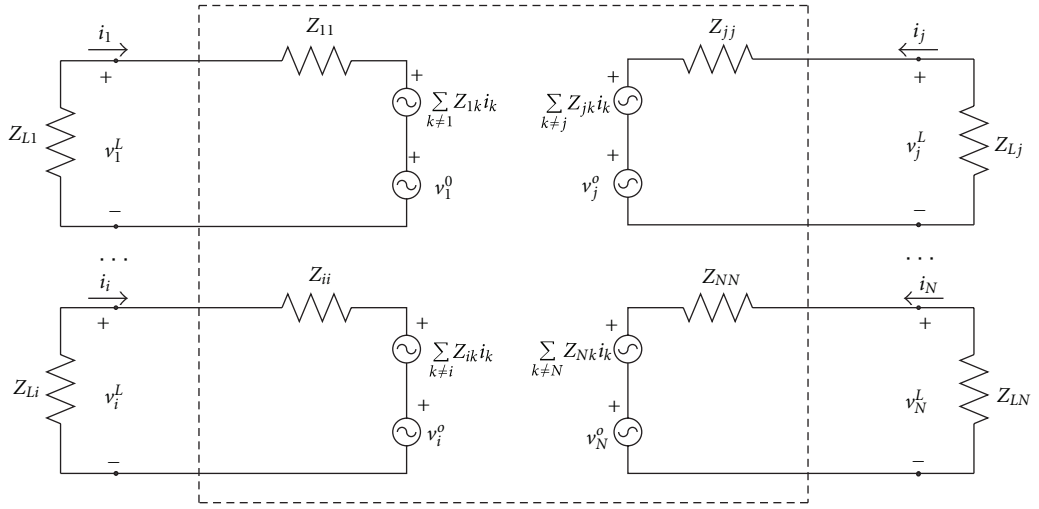

FIGURE 1: Circuit model for analyzing antenna coupling effects. Superscript "o" denotes open circuit voltage, and subscripts i, j denote particular elements of the array. Z_L is the load impedance, N is the total number of antennas.

with complex antenna structures or irregular arrangement. Therefore, we need to develop a new and feasible way to compensate for the antenna mutual coupling effect in imaging applications of the large interferometric array radiometers.

3. An External Calibration Method for Compensating for the Mutual Coupling Effect

3.1. The Visibility Model Including Antenna Mutual Coupling Effect. In order to point out the significance of (3), let us consider a simple case of a two-element array satisfying $Z_{11} = Z_{22}$, $Z_{12} = Z_{21}$, and $Z_{L1} = Z_{L2} = Z_L$. With these assumptions, the visibility sample that would be measured between antennas 1-1, V_{11}^L, and between antennas 1-2, V_{12}^L, can be computed from (3) as:

$$\begin{aligned} V_{12}^L &= \frac{1}{\left|(1+(Z_{11}/Z_L))^2-(Z_{12}/Z_L^2)\right|^2} \\ &\quad\times\left\{-2\Re\left[\left(1+\frac{Z_{11}}{Z_L}\right)\frac{Z_{12}^*}{Z_L^*}\right]T_A+\left|\frac{Z_{12}}{Z_L}\right|^2 V_{12}^{o^*}\right. \\ &\quad\left.+\left|1+\frac{Z_{11}}{Z_L}\right|^2 V_{12}^o\right\} \\ &= a_0 V_{12}^o + a_1 T_A + a_2 V_{12}^{o^*}, \\ V_{11}^L &= \frac{1}{\left|(1+(Z_{11}/Z_L))^2-(Z_{12}/Z_L^2)\right|^2} \\ &\quad\times\left\{-2\Re\left[\left(1+\frac{Z_{11}}{Z_L}\right)\frac{Z_{12}^*}{Z_L^*}V_{12}^o\right]\right. \\ &\quad\left.+\left[\left|\frac{Z_{12}}{Z_L}\right|^2+\left|1+\frac{Z_{11}}{Z_L}\right|^2\right]T_A\right\} \\ &= b_0 T_A + \Re[b_1 V_{12}^o], \end{aligned} \tag{4,5}$$

where $\Re[\bullet]$ denotes the real-part operation, $V_{11}^o = V_{22}^o = T_A$ is used; and the coefficients

$$\begin{aligned} a_0 &= \frac{|1+(Z_{11}/Z_L)|^2}{\left|(1+(Z_{11}/Z_L))^2-(Z_{12}/Z_L^2)\right|^2}, \\ a_1 &= \frac{-2\Re\left[(1+(Z_{11}/Z_L))(Z_{12}^*/Z_L^*)\right]}{\left|(1+(Z_{11}/Z_L))^2-(Z_{12}/Z_L^2)\right|^2}, \\ a_2 &= \frac{|Z_{12}/Z_L|^2}{\left|(1+(Z_{11}/Z_L))^2-(Z_{12}/Z_L^2)\right|^2}, \\ b_0 &= \frac{\left[|Z_{12}/Z_L|^2+|1+(Z_{11}/Z_L)|^2\right]}{\left|(1+(Z_{11}/Z_L))^2-(Z_{12}/Z_L^2)\right|^2}, \\ b_1 &= \frac{-2\left[(1+(Z_{11}/Z_L))(Z_{12}^*/Z_L^*)\right]}{\left|(1+(Z_{11}/Z_L))^2-(Z_{12}/Z_L^2)\right|^2}. \end{aligned} \tag{6}$$

In the following analysis, we assume that (1) $Z_{12} \ll Z_{11}$ and Z_{12} decreases with the inverse of the antenna spacing and (2) $T_A \gg |V_{12}^0|$ (this often holds true for Earth observation). With these assumptions, we have $a_0 \gg a_1 \gg a_2$ and $b_0 \gg |b_1|$. Therefore, from (4) and (5), we come to the conclusions: (1) the measured cross-correlation sample V_{12}^L can be approximately considered as the ideal one plus an offset term proportional to antenna temperature T_A; (2) the measured zero-spacing visibility sample V_{11}^L is approximately constant because the additional spatial frequency term in (5) is very small compared to the constant term $b_0 T_A$ and hence can be neglected. Similar conclusions are hold when the two-element array is extended to a more general case. In fact, the antenna mutual coupling effect needs to be considered between only a few adjacent antennas in the thinned interferometric arrays as the mutual impedance decreases with the

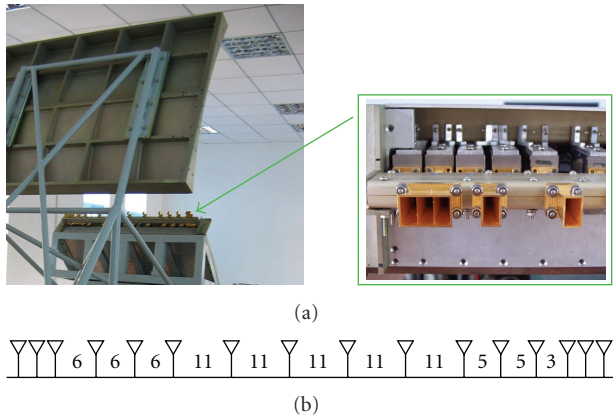

(a)

(b)

Figure 2: The HUST-ASR antenna array; (a) the photo of the whole antenna and the partial feed array; (b) a 16-element minimum redundancy linear feed array which can simultaneously measure visibility at 91 contiguous spacings (including zero spacing) with just 16 antennas. According to this arrangement, a conjoined triple-horn structure has to be used at each end of the array because of the very close spacings which contribute much to the mutual coupling.

inverse of the antenna spacing. The above conclusions will help us to develop model of the coupled visibility.

For an ideal one-dimensional aperture synthesis radiometer, the visibility function $V(u)$ and the brightness temperature distribution $T_B(\xi)$ are related by a Fourier Transformation [1, 3]

$$V(u) = K \int_{-1}^{1} T_B(\xi) e^{-j2\pi u\xi} d\xi, \tag{7}$$

where K is a constant term related to antenna and channel parameters, u is the spatial frequency equal to the spacing between a given antenna pair normalized by the wavelength, $\xi = \sin\theta$ is the direction cosine, $\theta \in [-\pi/2,\ \pi/2]$ is the angle away from the normal of array axis. Ideally, each sample of the visibility function is a measure of a spatial harmonic in the brightness temperature scene.

Following the above conclusions, the antenna mutual coupling effect can be represented by an additive term to the ideal visibility sample. And considering the noise-like characteristic of the interferometric measurement, the effect of antenna mutual coupling on the measured visibility sample can be modeled as

$$V^{\text{raw}}(u) = K \int_{-1}^{1} T_B(\xi) e^{-j2\pi u\xi} d\xi + V^{\text{add}}(u) + w^{\text{raw}}(u), \tag{8}$$

where $V^{\text{raw}}(u)$ is the measured visibility sample including antenna coupling, $V^{\text{add}}(u)$ is an additive error on the ideal visibilities accounting for the antenna mutual coupling effect and only depends on the array parameters and antenna temperature T_{A}, and $w^{\text{raw}}(u)$ is the random measurement noise on the visibility sample.

3.2. External Calibration Process via the "Difference Scene Measurement." Since the additive error $V^{\text{add}}(u)$ is independent on the scene brightness temperature distribution $T_{\text{B}}(\xi)$ within the FOV, it is possible to remove it via the difference measurement between the original scene and a known reference scene. Inspiring from this, we develop an external calibration process given below to compensate for the antenna mutual coupling effect.

First, we measure the original scene and obtain the raw visibilities expressed as (8). In practice, the raw visibilities in (8) are measured at the discrete spatial frequencies and can be written as the following matrix formation:

$$\mathbf{V}^{\text{raw}} = \mathbf{F}\mathbf{T} + \mathbf{V}^{\text{add}} + \mathbf{w}^{\text{raw}}, \tag{9}$$

where $\mathbf{V}^{\text{raw}} = [V_1^{\text{raw}}, V_2^{\text{raw}}, \ldots, V_P^{\text{raw}}]^T$, $P = 2M+1$, M is the maximum spatial frequency (i.e., the array length normalized by the minimum spacing); $\mathbf{F}$ is Fourier transformation operator, $\mathbf{T} = [T_1, T_2, \ldots, T_P]^T$ is the scene brightness temperature vector divided into P pixels within the non-aliasing FOV, $\mathbf{V}^{\text{add}} = [V_1^{\text{add}}, V_2^{\text{add}}, \ldots, V_P^{\text{add}}]^T$ is the additive visibility error vector due to antenna mutual coupling, $\mathbf{w}^{\text{raw}} = [w_1^{\text{raw}}, w_2^{\text{raw}}, \ldots, w_P^{\text{raw}}]^T$ is the random measurement noise vector for the original scene.

Second, we choose a naturally occurring scene with a uniform brightness temperature distribution (e.g., the cold sky, the anechoic chamber, the open water, etc.) as a reference scene and measure its visibilities under the same hardware situation. Similar to (9), the measured visibilities of the reference scene, $\mathbf{V}^{\text{ref}}$, can be expressed as

$$\mathbf{V}^{\text{ref}} = \mathbf{F}T^{\text{ref}} \cdot \mathbf{I}_P + \mathbf{V}^{\text{add}} + \mathbf{w}^{\text{ref}}, \tag{10}$$

where T^{ref} is the brightness temperature distribution of the uniform reference scene, $\mathbf{I}_P$ is a P-dimensional unit vector, $\mathbf{V}^{\text{add}}$ is the same as that in (9) due to the same antenna coupling and the same measurement situation, and $\mathbf{w}^{\text{ref}}$ is the random measurement noise for the reference scene.

Then, by subtracting (10) from (9), we can get the calibrated visibilities (i.e., the decoupled visibilities)

$$\mathbf{V}^{\text{cal}} = \mathbf{V}^{\text{raw}} - \mathbf{V}^{\text{ref}} = \mathbf{F}\mathbf{T}^{\text{diff}} + \mathbf{w}^{\text{raw}} + \mathbf{w}^{\text{ref}}, \tag{11}$$

where $\mathbf{T}^{\text{diff}} = [T_1 - T^{\text{ref}}, T_2 - T^{\text{ref}}, \ldots, T_P - T^{\text{ref}}]^T$ is the difference brightness temperature vector. Equation (11) shows that the additive error term resulting from antenna mutual coupling, $\mathbf{V}^{\text{add}}$, can be removed through the difference measurement between the original scene and the reference scene.

The essence of the "difference scene measurement" method lies in the decreased noise in the measured visibilities and therefore in the inverted images. For the ideal measurement without antenna imperfections, the cross-correlation matrix of the visibility is

$$\begin{aligned} \mathbf{C}_{\mathbf{V}} &= E\left[\Delta\mathbf{V}\Delta\mathbf{V}^H\right] \\ &= E\left[\mathbf{w}^{\text{raw}}(\mathbf{w}^{\text{raw}})^H\right], \end{aligned} \tag{12}$$

where $E[\bullet]$ denotes the mathematical expectation. Since the brightness temperature image is obtained by means of a discrete Fourier transform of the visibility samples, the cross-correlation matrix of the image can be calculated by [22]

$$\mathbf{C}_T = \mathbf{F}^{-1}\mathbf{C}_{\mathbf{V}}(\mathbf{F}^{-1})^H. \tag{13}$$

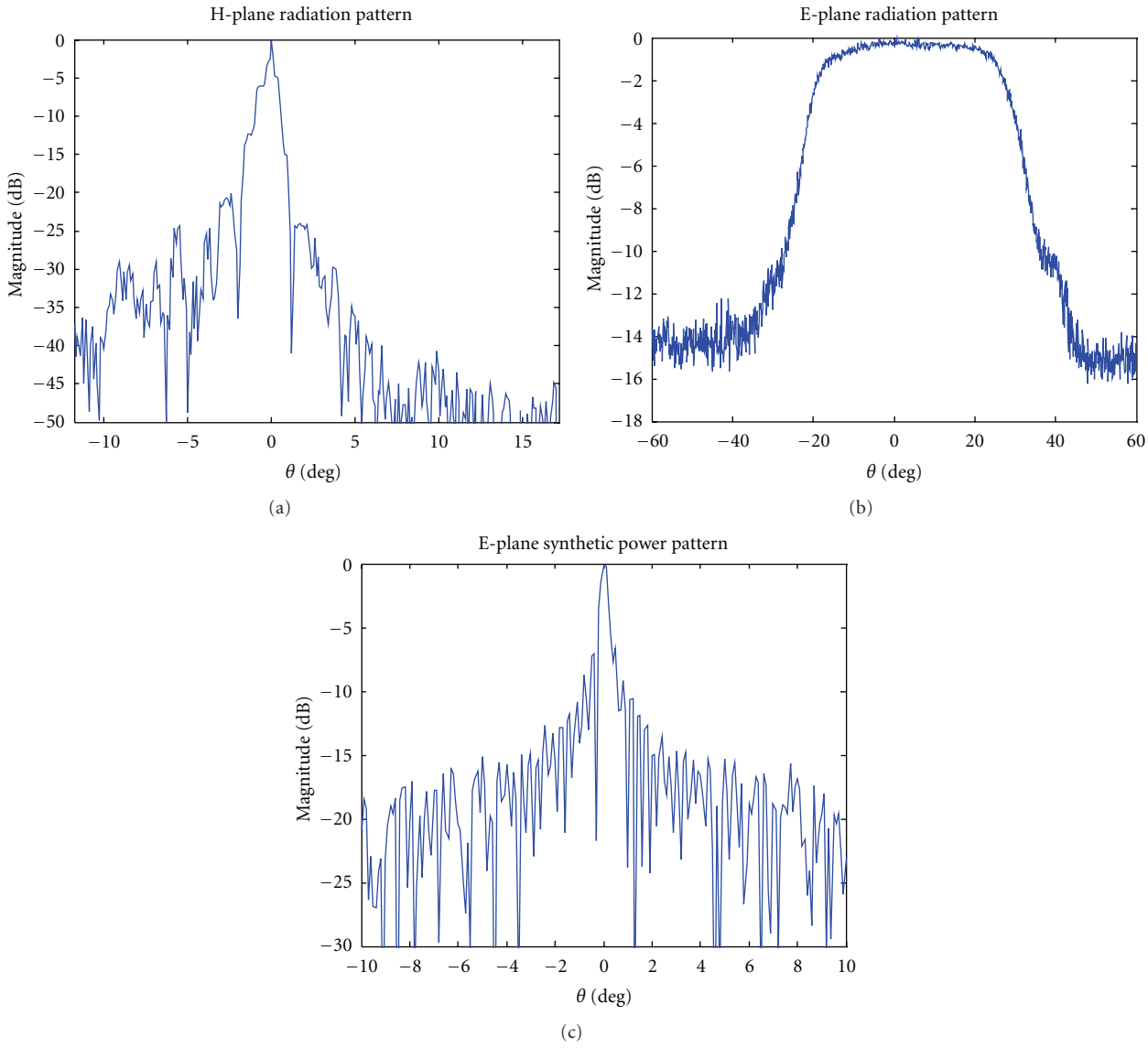

Figure 3: The measured HUST-ASR antenna pattern: (a) the H-plane pattern of an "element"; (b) the E-plane pattern of an "element"; (c) the synthesized E-plane pattern of all the "elements" by interferometric aperture synthesis.

Equation (13) shows that the noise (or errors) in the measured visibilities can be transferred to the inverted images.

With the antenna mutual coupling effect, the crosscorrelation matrix of the visibility

$$\begin{aligned}\mathbf{C}_V^{\mathrm{mu}} &= E\left[\left(\mathbf{V}^{\mathrm{add}}+\mathbf{w}^{\mathrm{raw}}\right)\left(\mathbf{V}^{\mathrm{add}}+\mathbf{w}^{\mathrm{raw}}\right)^H\right] \\ &= E\left[\mathbf{V}^{\mathrm{add}}\left(\mathbf{V}^{\mathrm{add}}\right)^H\right]+E\left[\mathbf{w}^{\mathrm{raw}}\mathbf{w}^{\mathrm{raw}H}\right],\end{aligned} \tag{14}$$

assuming the measurement noise and the additive visibility error are unrelated. Equation (14) shows that the noise variance of the measured visibilities increases when the antenna mutual coupling is included. By introducing the "difference scene measurement," the cross-correlation matrix of the visibility

$$\begin{aligned}\mathbf{C}_V^{\mathrm{diff}} &= E\left[\left(\mathbf{w}^{\mathrm{raw}}+\mathbf{w}^{\mathrm{ref}}\right)\left(\mathbf{w}^{\mathrm{raw}}+\mathbf{w}^{\mathrm{ref}}\right)^H\right] \\ &= E\left[\mathbf{w}^{\mathrm{raw}}(\mathbf{w}^{\mathrm{raw}})^H\right]+E\left[\mathbf{w}^{\mathrm{ref}}\left(\mathbf{w}^{\mathrm{ref}}\right)^H\right]\end{aligned} \tag{15}$$

assuming the measurement noise for the original scene and measurement noise for the reference scene are unrelated. The comparison between (14) and (15) shows that for the "difference scene measurement" method, the additive visibility error resulting from antenna mutual coupling is removed at the cost of the increased random measurement noise. Fortunately, this increase in the calibrated visibilities

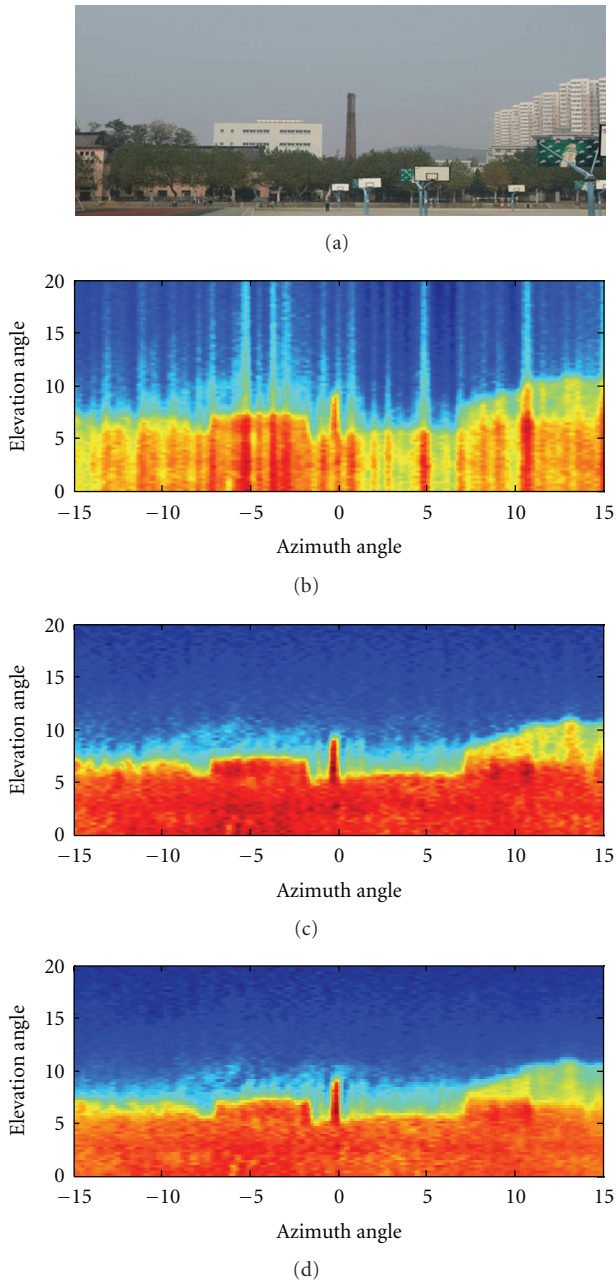

FIGURE 4: Images of the campus playground within a wide FOV; (a) optic image; (b) the original brightness temperature image without mutual coupling compensation; (c) the calibrated brightness temperature image using the "difference scene measurement" method; (d) the calibrated brightness temperature image using the G-matrix method.

can be mitigated to the largest extent as long as the integration time for the reference scene is enough.

Finally, by inverting the decoupled visibilities $\mathbf{V}^{\text{cal}}$, we can get the difference brightness temperature distribution $\mathbf{T}^{\text{diff}}$ (this relative brightness temperature is usually enough for many imaging applications). Since T^{ref} is usually a constant and can be exactly measured, the original scene brightness temperature distribution $\mathbf{T}$ can be easily recovered.

Compared with the previous methods such as the G-matrix method and the mutual impedance method, the proposed method is fast and simple for adapting to the Fourier-based inversion techniques. Furthermore, the decoupled procedures on the measured visibilities require no extra hardware cost and have easier implementation, which makes the method most attractive for imaging applications of the large interferometric array radiometers.

4. Experiment Results

To validate the effectiveness of our approach, a series of imaging experiments were carried out with the HUST-ASR [23], which is a prototype of one-dimensional interferometric aperture synthesis radiometer (IASR) working at 8-mm wave band. One-dimensional IASR requires antennas to produce a group of fan-beams which overlap and can be interfered with each other to synthesize multiple pencil beams simultaneously. According to this requirement, the HUST-ASR antenna system [24], as shown in Figure 2, is a sparse antenna array with an offset parabolic cylinder reflector. The feed horns are sparsely arranged in a minimum redundancy linear array [24–26] (as shown in Figure 2(b)) along the focal line of the reflector, and thus can share a single offset parabolic cylinder reflector. In essence, each HUST-ASR antenna "element" is composed of a feed horn and an offset parabolic cylinder reflector with a gain of about 30 dB. The H-plane (i.e., the vertical plane) and E-plane (i.e., horizontal plane) radiation patterns of one "element" are presented in Figures 3(a) and 3(b), showing that the half-power beamwidths (HPBWs) of the H-plane and E-plane are about 0.7° and 50°, respectively.

With this configuration, the HUST-ASR can synthesize a series of pencil beams with about 0.3° HPBW (as shown in Figure 3(c)) by interference processing in the E-plane, and therefore generate a one-dimensional image with high spatial resolution. In order to generate a two-dimensional high resolution image, a rotation platform is used to provide a mechanic scan at another dimension. Figure 4 shows the brightness temperature images of natural scenes. In this figure, the original brightness temperature image without mutual coupling compensation, the calibrated image using the proposed "difference scene measurement," and the calibrated image using the G-matrix method are presented, respectively.

In Figure 4(b), the original brightness temperature image was contaminated with some vertical "streaks" due to the mutual coupling effect between close antennas. This confirms the correctness of the coupled visibilities model given in Section 3.1. In Figure 4(c), these "streaks" are almost removed by using the proposed method and the outline of the chimney and the buildings can be clearly seen in the images. In our experiments, the cold sky is used as a smooth reference scene to cancel the antenna coupling effect. In Figure 4(d), the image obtained by the G-matrix method is also presented. Compared to Figure 4(c), the brightness temperature at the edge of the scene seems a bit dim because the farther away from the boresight, the weaker the G-matrix response is. The experimental results demonstrate the

effectiveness of the proposed method in dealing with antenna coupling errors, and the calibrated image obtained by the proposed method is completely comparable to that obtained by the G-matrix method. Considering the fact that the G-matrix method needs extra hardware cost and large computational load and the inaccurate G-matrix measurement may introduce new errors in the final image, the proposed method in this paper provides an attractive candidate for imaging applications of the large interferometric array radiometers.

Besides, the slow transition from high brightness temperature zone to low brightness temperature zone can be clearly seen in the images especially at the low elevation angle due to the sidelobe effect in the H-plane pattern. Thus, further work needs to be done on minimizing sidelobe levels in the H-plane pattern.

5. Conclusion

In this paper, we have investigated the mutual coupling effect in interferometric aperture synthesis radiometers (IASRs) using the conventional mutual impedance (CMI), which reveals that the coupled visibilities are a linear combination of all the ideal visibilities that can be synthesized by the array. Then, we have developed a practical model of the coupled visibilities. In this model, the antenna mutual coupling effect on the measured visibility samples can be represented by an additive term to the ideal visibility samples which is only dependent on the array parameters and antenna temperature. Based on the model, we propose an external calibration method to compensate for the antenna mutual coupling effect. In this method, the measured visibilities are decoupled through the difference in measurement between the original scene and a naturally occurring reference scene. Theoretical analysis on the cross-correlation matrix of the visibility shows that the proposed method can effectively reduce the noise in the measured visibilities and therefore in the inverted images. In addition to theoretical studies, we have experimentally demonstrated the effectiveness of the proposed method in compensating for the antenna mutual coupling effect. Compared to the previous methods, the proposed method requires no additional hardware cost and has easier implementation, which is most attractive for imaging applications of the large interferometric array radiometers.

Recently, a new model for antenna mutual coupling characterization, the receiving mutual impedance (RMI) [27–29], is proposed and shows the superiority over the CMI in passive receiving array mode (e.g., the IASR system). Thus, future work will be aimed at applying the RMI to model the antenna mutual coupling effect on the performance of IASR and developing new methods for compensating for the mutual coupling effect.

Acknowledgments

This work was supported in part by the Central South University (CSU) under Grants no. 2011QNZT031, no. 74341015812, and no. 201109Y18 and in part by the Huazhong University of Science and Technology (HUST) under Grant no. 40806069. The authors would like to thank Professors Wei Guo, Fei Hu, and Quanliang Huang for their enthusiastic encouragements. The authors also thank the work of Dr. Rong Jin, Dr. Liangbin Chen, and Dr. Fangmin He in helping to perform experiments and develop the processing code. The authors also thank Handong Wu, Yingying Wang in Xi'an Hengda Microwave Technology Corp. for their contributions to the HUST-ASR.

References

[1] A. R. Thompson, J. M. Morgan, J. George, and W. Swenson, *Interferometry and Synthesis in Radio Astronomy*, John Wiley & Sons, New York, NY, USA, 2nd edition, 2001.

[2] D. M. Le Vine and J. C. Good, "Aperture synthesis for microwave radiometry in space," NASA Technical Memorandum 85033, 1983.

[3] C. S. Ruf, C. T. Swift, A. B. Tanner, and D. M. Le Vine, "Interferometric synthetic aperture microwave radiometry for the remote sensing of the earth," *IEEE Transactions on Geoscience and Remote Sensing*, vol. 26, no. 5, pp. 597–611, 1988.

[4] A. S. Milman, "Sparse-aperture microwave radiometers for earth remote sensing," *Radio Science*, vol. 23, no. 2, pp. 193–205, 1988.

[5] C. T. Swift, D. M. Le Vine, and C. S. Ruf, "Aperture synthesis concepts in microwave remote sensing of the earth," *IEEE Transactions on Microwave Theory and Techniques*, vol. 39, no. 12, pp. 1931–1935, 1991.

[6] F. T. Ulaby, R. K. Moore, and A. K. Fung, *Microwave Remote Sensing Fundamentals and Radiometry*, vol. 1, Addison-Wesley Publishing Company, Massachusetts, Boston, 1981.

[7] A. Camps, *Application of interferometric radiometry to Earth observation*, Ph.D. dissertation, Universitat Politècnica de Catalunya, Barcelona, Spain, 1996.

[8] C. S. Ruf, "Error analysis of image reconstruction by a synthetic aperture interferometric radiometer," *Radio Science*, vol. 26, no. 6, pp. 1419–1434, 1991.

[9] A. B. Tanner and C. T. Swift, "Calibration of a synthetic aperture radiometer," *IEEE Transactions on Geoscience and Remote Sensing*, vol. 31, no. 1, pp. 257–267, 1993.

[10] M. Martín-Neria and J. M. Goutoule, "A two-dimensional aperture-synthesis radiometer for soil-moisture and ocean-salinity observations," *ESA Bulletin*, vol. 92, pp. 95–104, 1997.

[11] I. Corbella, F. Torres, N. Duffo et al., "On-ground characterization of the SMOS payload," *IEEE Transactions on Geoscience and Remote Sensing*, vol. 47, no. 9, pp. 3123–3133, 2009.

[12] B. Lambrigtsen, W. Wilson, A. B. Tanner, T. Gaier, C. S. Ruf, and J. Piepmeier, "GeoSTAR—a microwave sounder for geostationary satellites," in *Proceedings of the IEEE International Geoscience and Remote Sensing Symposium (IGARSS '04)*, vol. 2, pp. 777–780, 2004.

[13] F. Torres, A. B. Tanner, S. T. Brown, and B. H. Lambrigsten, "Robust array configuration for a microwave interferometric radiometer: application to the GeoSTAR project," *IEEE Geoscience and Remote Sensing Letters*, vol. 4, no. 1, pp. 97–101, 2007.

[14] D. M. Le Vine and D. E. Weissman, "Calibration of synthetic aperture radiometers in space: antenna effects," in *Proceedings*

of the International Geoscience and Remote Sensing Symposium (IGARSS '96), pp. 878–880, Lincoln, Nebraska, 1996.

[15] D. E. Weissman and D. M. Le Vine, "The role of mutual coupling in the performance of synthetic aperture radiometers," *Radio Science*, vol. 33, no. 3, pp. 767–779, 1998.

[16] A. Camps, J. Bará, F. Torres, I. Corbella, and J. Romeu, "Impact of antenna errors on the radiometric accuracy of large aperture synthesis radiometers," *Radio Science*, vol. 32, no. 2, pp. 657–668, 1997.

[17] A. Camps, J. Bará, F. Torres, I. Corbella, and J. Romeu, "Mutual coupling effects on antenna radiation pattern: an experimental study applied to interferometric radiometers," *Radio Science*, vol. 33, no. 6, pp. 1543–1552, 1998.

[18] R. E. Collin and F. J. Zucker, *Antenna Theory*, McGraw-Hill, New York, NY, USA, 1968.

[19] I. J. Gupta and A. A. Ksienski, "Effect of mutual coupling on the performance of adaptive arrays," *IEEE Transactions on Antennas and Propagation*, vol. 31, no. 5, pp. 785–791, 1983.

[20] C.-C. Yeh, M.-L. Leou, and D. R. Ucci, "Bearing estimations with mutual coupling present," *IEEE Transactions on Antennas and Propagation*, vol. 37, no. 10, pp. 1332–1335, 1989.

[21] J. Bará, A. Camps, F. A. Torres, and I. Corbella, "The correlation of visibility noise and its impact on the radiometric resolution of an aperture synthesis interferometric radiometry," *IEEE Transactions on Geoscience and Remote Sensing*, vol. 38, no. 5, pp. 2423–2426, 2000.

[22] R. Butora and A. Camps, "Noise maps in aperture synthesis radiometric images due to cross-correlation of visibility noise," *Radio Science*, vol. 38, no. 4, pp. 1067–1074, 2003.

[23] Q. Li, F. Hu, W. Guo et al., "A general platform for millimeter wave synthetic aperture radiometers," in *Proceedings of the IEEE International Geoscience and Remote Sensing Symposium (IGARSS '08)*, vol. 2, pp. 1156–1159, 2008.

[24] J. Dong, Q. Li, W. Guo, and Y. Zhu, "A sparse antenna array with offset parabolic cylinder reflector at millimeter wave band," in *Proceedings of the IEEE International Conference on Material and Manufacturing Technology (ICMMT '08)*, vol. 4, pp. 1667–1670, 2008.

[25] J. Dong, Q. Li, R. Jin, Y. Zhu, Q. Huang, and L. Gui, "A method for seeking low-redundancy large linear arrays in aperture synthesis microwave radiometers," *IEEE Transactions on Antennas and Propagation*, vol. 58, no. 6, pp. 1913–1921, 2010.

[26] J. Dong, L. Qingxia, S. Ronghua, G. Liangqi, and G. Wei, "The placement of antenna elements in aperture synthesis microwave radiometers for optimum radiometric sensitivity," *IEEE Transactions on Antennas and Propagation*, vol. 59, no. 11, 2011.

[27] H. T. Hui, "A practical approach to compensate for the mutual coupling effect in an adaptive dipole array," *IEEE Transactions on Antennas and Propagation*, vol. 52, no. 5, pp. 1262–1269, 2004.

[28] H. T. Hui, "Improved compensation for the mutual coupling effect in a dipole array for direction finding," *IEEE Transactions on Antennas and Propagation*, vol. 51, no. 9, pp. 2498–2503, 2003.

[29] H. S. Lui and H. T. Hui, "Mutual coupling compensation for direction-of-arrival estimations using the receiving-mutual-impedance method," *International Journal of Antennas and Propagation, Mutual Coupling in Antenna Arrays*, vol. 2010, pp. 1–7, 2010.